Detrital zircon evidence for derivation of arkosic sand in the eolilan Narbona Pass Member of the Eocene-Oligocene Chuska Sandstone from Precambrian basement rocks in central Arizona

William R. Dickinson, Steven M. Cather, and George E. Gehrels

2010, pp. 125-134. https://doi.org/10.56577/FFC-61.125

in:

Geology of the Four Corners Country, Fassett, James E.; Zeigler, Kate E.; Lueth, Virgil W., [eds.], New Mexico Geological Society 61 st Annual Fall Field Conference Guidebook, 246 p. https://doi.org/10.56577/FFC-61

This page is intentionally left blank to maintain order of facing pages.

New Mexico Geological Society Guidebook, 61st Field Conference, Four Corners Country, 2010, p. 125-134.

DETRITAL ZIRCON EVIDENCE FOR DERIVATION OF ARKOSIC SAND IN THE EOLIAN NARBONA PASS MEMBER OF THE EOCENE–OLIGOCENE CHUSKA SANDSTONE FROM PRECAMBRIAN BASEMENT ROCKS IN CENTRAL ARIZONA

WILLIAM R. DICKINSON[1], STEVEN M. CATHER[2], AND GEORGE E. GEHRELS[1]

[1]Department of Geosciences, University of Arizona, Tucson, AZ 85721, wrkickin@dakotacom.net
[2]New Mexico Bureau of Geology and Mineral Resources, 801 Leroy Place, Socorro, NM 87801

ABSTRACT—The Narbona Pass Member of the Chuska Sandstone, exposed only along the crest of the Chuska Mountains (Arizona–New Mexico), is the central remnant of the Oligocene Chuska erg, which is inferred to have occupied ~125,000 km^2 of the southeastern Colorado Plateau within a subcircular area surrounded by Oligocene volcanic fields. The high paleotopography of active volcanic edifices delimited the lateral extent of erg deposition except to the west, which was upwind for eolian sand transport. The dominant arkosic petrofacies of the Narbona Pass Member, as exposed at Narbona Pass near Crystal (NM) and at Buffalo Pass near Lukachukai (AZ), was derived mainly from Precambrian basement in central Arizona. The principal subpopulations of detrital zircons (n=100 grains) by U-Pb age are 1770-1640 Ma (~70% with age peak at 1700 Ma), reflecting derivation from the Yavapai-Mazatzal belt of southwest Laurentia, and 1460-1400 Ma (~15% with age peak at 1425 Ma) derived from anorogenic granite bodies intrusive into Yavapai-Mazatzal basement. Precambrian detritus was apparently carried northward to alluvial plains deposited west of the Chuska erg and deflated to feed sand into the erg interior. Other remnants of the Chuska erg along the northern flank of the Mogollon-Datil volcanic field, in the subsurface of the Albuquerque basin of the Rio Grande rift, and near Whiskey Lake in the southernmost Chuska Mountains are petrographically distinct from the arkosic petrofacies of the erg interior, and were evidently derived from other sources as yet untested by detrital zircons. The areal variability of erg sand implies either different pathways for sand transport across the expanse of an integrated Chuska erg or segmentation of the Chuska erg into multiple subdivisions that were partly separated by inselbergs of the pre-Oligocene erg substratum.

INTRODUCTION

The Oligocene Chuska erg, with a reconstructed subcircular extent of ~125 x 10^3 km^2 on the Colorado Plateau (Fig. 1), was the largest Cenozoic sand sea for which any remnant is preserved in North America (Cather et al., 2008). The central remnant of the erg forms the Narbona Pass Member (Lucas and Cather, 2003) of the Chuska Sandstone exposed over an elongate area of ~1000 km^2 along the crest of the Chuska Mountains spanning the Arizona–New Mexico border (Fig. 1). Erg deposits reached a thickness of at least 535 m at Roof Butte between Lukachukai (AZ) and Shiprock (NM). The Chuska erg occupied a broad tract of subdued paleotopography bounded on the north, east, and south by Oligocene volcanic fields (Fig. 1), which apparently built volcanic edifices high enough to confine eolian sand accumulation to the southeastern Colorado Plateau. Paleowinds blew eolian sand into and across the erg from sources to the west-southwest (Cather et al., 2003). We use the U-Pb ages of detrital zircon grains, supplemented by petrographic study, to infer the origin of the eolian sand in the Chuska erg.

Our study has inherent limitations because we determined U-Pb ages for just 100 detrital zircons from only one sample of eolian sand collected from the central Chuska Mountains (see locality information in the Appendix), and we outline cogent reasons to believe that the eolian sand in other parts of the Chuska erg had different origins. Our U-Pb data pertain only to sand in the central Chuska erg for which the U-Pb ages of detrital zircons imply ultimate derivation from Precambrian source rocks in central Arizona. Preliminary U-Pb data were presented by Eichler and McGraw (2008), but reanalysis of the zircon grains for this study improved the accuracy and precision of the U-Pb ages (Dickinson et al., 2009a), which are presented in the Appendix.

METHODOLOGY

U-Pb ages of detrital zircons have become a standard tool for studies of sand provenance (Dickinson and Gehrels, 2009b), and commonly reveal information about bedrock sources for sand that cannot be obtained from petrographic or paleocurrent studies. Zircon, although it is subordinate volumetrically in sand, is a convenient proxy for accompanying quartz and feldspar grains because the ultimate origins of all three minerals are principally felsic igneous and meta-igneous rocks. Placering can affect proportions of zircon and quartz-feldspar grains in sand, but sediment dispersal cannot readily mix zircon and quartz-feldspar grains from wholly disparate sources. Newly grown quartz and feldspar are also common in metasedimentary rocks, but zircon U-Pb ages are not reset by metamorphism below granulite grade. Consequently, U-Pb ages for detrital zircons reworked from metasedimentary rock commonly preserve a record of the provenance for the sediments before metamorphism. The persistence of zircon grains in the sedimentary environment also means that zircon grains can be recycled from sedimentary rock without changing the U-Pb age spectra of the recycled zircon grains (Dickinson et al., 2009b), and this factor must always be taken into account for provenance interpretations.

U-Pb ages of detrital zircon grains are reliable guides to the ages of the ultimate source rocks for the zircons precisely because the U-Pb ages are not reset by any diagenetic or by most metamorphic processes. Moreover, the twin decay schemes of ^{238}U (to

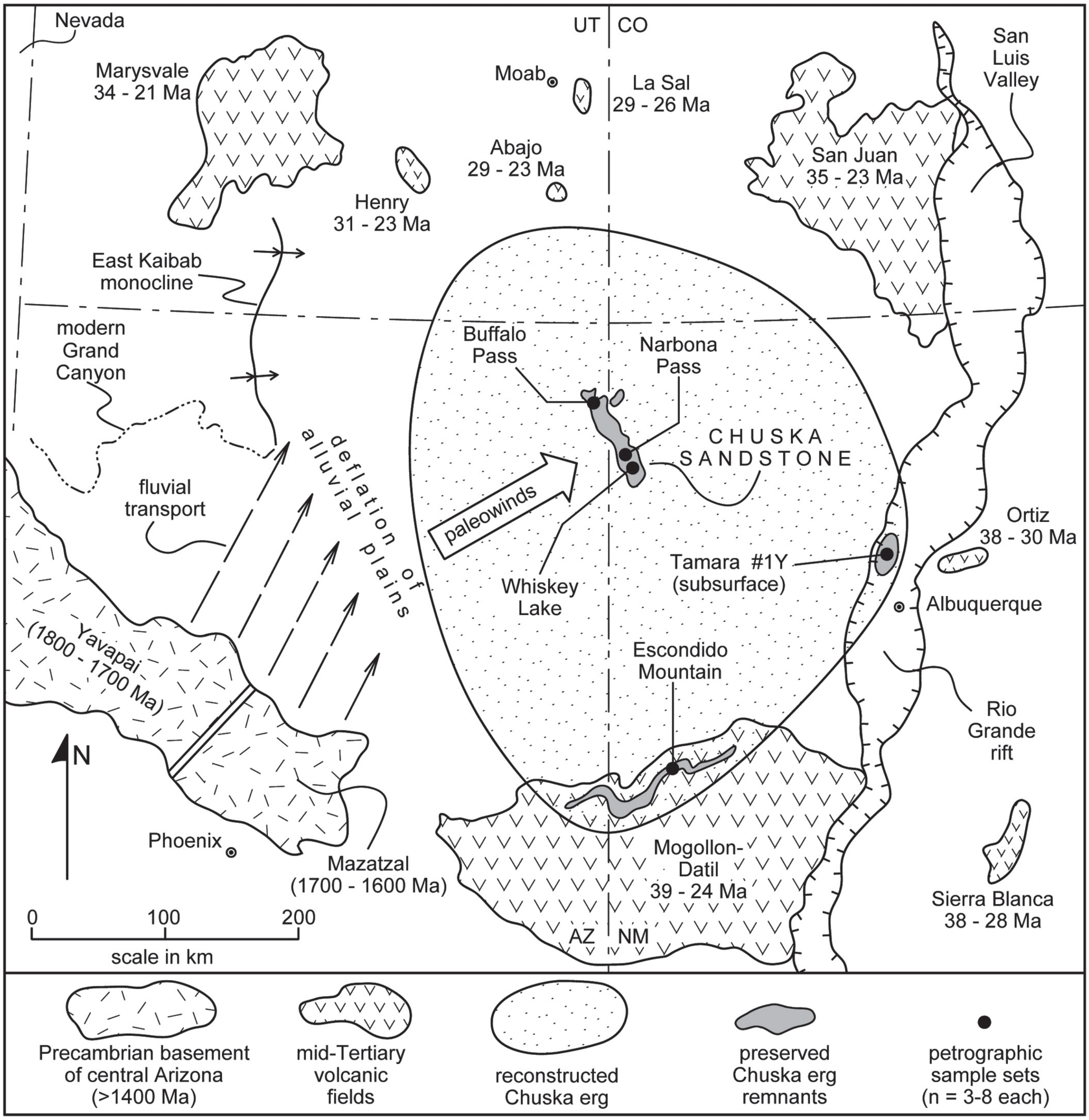

FIGURE 1. Plan view of the Chuska erg and its surroundings adapted after Cather et al. (2008). Yavapai–Mazatzal boundary after Shaw and Karlstrom (1999).

^{206}Pb) and ^{235}U (to ^{207}Pb) allow any disturbance to the U/Pb isotopic system (such as leaching of lead from crystals) to be detected by a discordance in ^{206}Pb/^{238}U and ^{207}Pb/^{235}U ages for the same zircon grain. In practice, the ages of detrital zircons yielding discordant ages are rejected for provenance analysis, and all the 100 U-Pb ages listed in the Appendix from the Chuska Sandstone are concordant or nearly so (within tight criteria limits). ^{206}Pb/^{238}U ages are preferred for grains <1 Ga, and ^{206}Pb/^{207}Pb ages for grains >1 Ga. No more than 5%-10% of U-Pb ages were rejected for discordance.

Our Chuska sample of well sorted and well rounded, medium-grained sandstone was collected as 20-25 kg of rock chips from which detrital zircons were separated by standard mineralogical techniques (crushing, grinding, Wilfley table, heavy liquids, Franz magnetic separator). Approximately 1000-2000 zircon grains were incorporated together with a Sri Lanka zircon standard into epoxy mounts, and dated individually by laser ablation and inductively coupled multicollector plasma-mass spectrometry (Gehrels et al., 2008). Grains for U-Pb analysis were selected randomly from the mounts, and every fifth firing of the laser beam was directed at a fragment of the zircon standard to correct for machine drift. The retention of grain mounts allows reappraisal of grain ages as analytical technology improves.

CHUSKA ERG STRATIGRAPHY

Figure 2 indicates the stratigraphic context of key remnants of the Chuska erg (Fig. 1). Strata underlying eolian deposits of the sand sea are dated isotopically near the Eocene–Oligocene time boundary, and overlying strata near the Oligocene–Miocene time boundary. Development of the Chuska erg was confined mainly or entirely to intervening Oligocene time. To the south, at the edge of the erg along the fringe of the Mogollon-Datil volcanic field, eolian deposits forming the local sandstone of Escondido Mountain (Chamberlin and Harris, 1994) interfinger with multiple ignimbrites. To the east, at the edge of the erg in the subsurface of the Rio Grande rift, eolian deposits in the unit of Isleta #2 are intercalated with fluvial deposits where penetrated in the Tamara #1-Y well, and the two are difficult to distinguish with confidence in well cuttings. In the central Chuska erg of the Chuska Mountains, eolian sandstone of the Narbona Pass Member of the Chuska Sandstone gradationally overlies fluvial sandstone of the Deza Member, displaying paleocurrent indicators of paleoflow toward the northeast near its base and toward the southwest near its top (Cather et al., 2003). The Narbona Pass Member forms an unbroken eolian facies >500 m thick that entirely buried and locally overstepped the fluvial Deza Member.

DETRITAL ZIRCON AGES

Figure 3 (top) is the age-distribution curve (age-probability plot of Ludwig, 2003) for detrital zircons in the Narbona Pass Member of the Chuska Sandstone near Narbona Pass (see Appendix for full U-Pb analytical data). The plot incorporates each U-Pb age with its analytical uncertainty as a normal distribution, then stacks the individual normal distributions into a single compound curve. The predominant grain-age peaks are at 1425 Ma and 1700 Ma (accounting jointly for nearly 90% of all the detrital zircons). The only other grain ages are three Mesozoic grains of ages (225-160 Ma) that are best explained by derivation from the Cordilleran magmatic arc of southwest Laurentia, single Paleozoic and Neoproterozoic grains of uncertain significance, and three grains each of Grenvillean (1000-1170 Ma) and Paleoproterozoic-Archean (1950-2820 Ma) age for which several alternate scenarios for fortuitous incorporation of odd persistent zircon grains into the sand are probably feasible.

Figure 3 (bottom) also includes the age-distribution curve for the closely comparable detrital-zircon population in a composite sample compounded of one sample each from the fluviodeltaic Upper Cretaceous (Turonian) Toreva Formation of the Black Mesa basin and Gallup Sandstone of the San Juan basin (Dickinson and Gehrels, 2008). The age-distribution curves for Chuska and Toreva-Gallup zircons are normalized to enclose the same sub-curve areas. Both Cretaceous units are known from paleocurrents and facies relations to derive from a provenance lying to the southwest of the Colorado Plateau (Cumella, 1983; Dickinson and Gehrels, 2008). The age-distribution curve for a sandstone sample from the younger Cretaceous (Campanian) Menefee Formation of the San Juan basin displays the same age peaks for detrital zircons of Precambrian age as the Toreva and Gallup samples (Dickinson and Gehrels, 2008), but Menefee detrital zircons also include 50% Mesozoic grains (<265 Ma) that make comparison with the Chuska detrital-zircon population less relevant.

The visual similarity of the Chuska and Toreva-Gallup age-distribution curves is strongly supported by Kolmogorov-Smirnoff (K-S) statistics (Press et al., 1986). K-S analysis takes all age

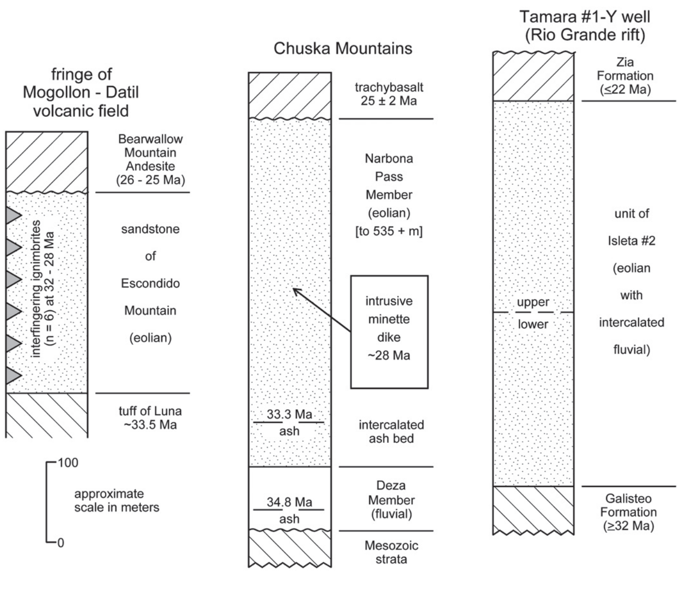

FIGURE 2. Stratigraphy of key remnants of Chuska erg (see Figure 1 for locations). Isotopic age constraints after Chamberlin and Harris (1994), Lucas and Cather (2003), and Cather et al. (2003, 2008).

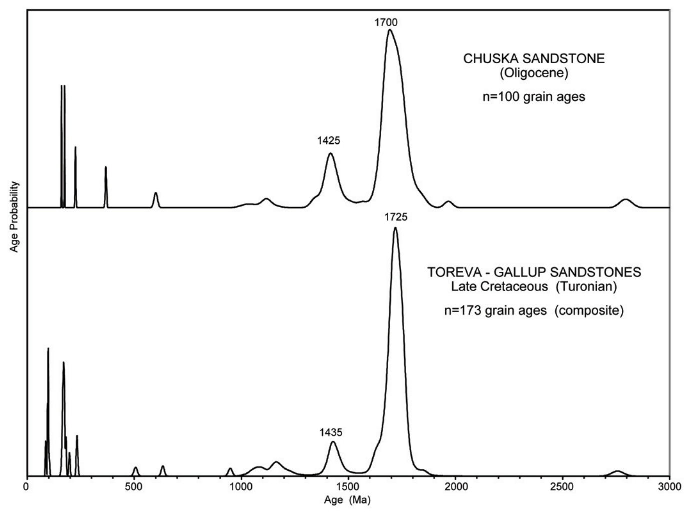

FIGURE 3. Age-distribution curves (see text) of detrital zircons in Narbona Pass Member of Chuska Sandstone (top) and Upper Cretaceous (Turonian) Toreva-Gallup sandstones (bottom) of Black Mesa and San Juan basins.

uncertainties in two detrital-zircon populations into account, and calculates a probability (P) that the two populations may have been derived from the same parent population by random choice of grains for analysis. Where P>0.05, there is <95% confidence that two observed populations do not derive from the same parent population, with P=0 indicating statistical identity. P=0.55 for comparison of the Chuska and Toreva-Gallup age spectra (Fig. 3), implying that the two age spectra are statistically indistinguishable for provenance interpretations. The reworking of zircon grains from Toreva-Gallup sources into the Chuska erg is not, however, a viable interpretation because Toreva-Gallup sandstones, though of similar grain size, are more quartzose (~75% quartz) than our sample of the Chuska Sandstone (~60% quartz). The content of resistant quartz relative to less resistant grain types is not expected to decline during recycling that involves some degree of weathering. Moreover, there is no expectation that Toreva-Gallup exposures were widespread enough in Oligocene time to yield the voluminous sand in the Chuska erg, and other Colorado Plateau Mesozoic units contain quite disparate detrital-zircon populations (Dickinson and Gehrels, 2008a, 2008b, 2009a).

Attention is drawn instead to derivation of the detrital zircons from a common provenance lying to the southwest of the depositional sites for both Toreva-Gallup and Chuska strata. The Precambrian basement of southwest Laurentia, as widely exposed in central Arizona (Karlstrom et al., 1987; Whitmeyer and Karlstrom, 2007), is composed of the orogenic Paleoproterozoic Yavapai (1800-1700 Ma) and Mazatzal (1700-1600 Ma) belts intruded by anorogenic Mesoproterozoic granitic plutons (1450-1400 Ma). These two components of the Arizona basement assemblage (Fig. 1) readily account for the 1700-1725 Ma and 1435-1425 Ma age peaks of the Chuska and Toreva-Gallup age-distribution curves (Fig. 2).

Modern ergs are most commonly nourished by sand deflated from playa lakes, riverine floodplains or alluvial fans, rather than by direct wind erosion of bedrock (Lancaster and Ollier, 1983; Wasson et al., 1983; Pell et al., 1997; Muhs et al., 2003). We accordingly infer that the central part of the Chuska erg received its sand supply from deflation of a now-eroded piedmont fluvial ramp built northward from Precambrian outcrops in central Arizona into a position just upwind from the Chuska erg (Fig. 1). The distribution of Yavapai and Mazatzal basement in central Arizona (Fig. 1) is appropriate to generate the joint Yavapai-Mazatzal age peak of 1700 Ma for Chuska detrital zircons. A suggestion (Cather et al., 2003) that volcanic rocks of the mid-Tertiary San Juan volcanic field (Fig. 1) may have contributed volcaniclastic detritus to Chuska eolianite forming the Narbona Pass Member, by reworking of sand from the underlying fluvial Deza Member, is discounted because not a single Cenozoic zircon grain was detected in our Narbona Pass sample. By contrast, half the detrital zircons in the modern Great Sand Dunes of Colorado, composed of largely volcanic sand (Wiegand, 1977) blown off alluvium derived in part from the San Juan volcanic field, are of Oligocene age (Madole et al., 2007). The U-Pb ages of detrital zircons in the Great Sand Dunes show that polygenetic volcanic fields which include silicic ignimbrites yield abundant zircon sand grains to derivative sediment.

CHUSKA ERG PETROFACIES

The Chuska eolianite sample from which we extracted detrital zircons is arkosic sandstone (Table 1), composed of grain types appropriate for sand derived mainly from granitoid basement rocks. The low P/K ratio (P/F=0.32) is characteristic of plutonic rather than volcanic sources for feldspar (Dickinson, 1985). Six other eolianite samples from the Narbona Pass Member of the Chuska Sandstone collected near Narbona Pass and at Buffalo Pass (Fig. 1) are similar arkosic sandstones (Table 2A) that cluster closely with our detrital zircon sample on a standard QmFLt ternary diagram (Fig. 4). Other sandstone samples from the Chuska erg differ markedly in modal composition from the arkosic petrofacies of the central Chuska erg at Narbona Pass and Buffalo Pass (Table 2; Fig. 4). For example, samples of the Narbona Pass Member from near Whiskey Lake (Fig. 1) in the southern Chuska Mountains are distinctly more quartzose (Table 2A) and resemble compositionally, although not texturally, sandstones in the underlying fluvial Deza Member of the Chuska Sandstone (Table 2B).

Samples from the sandstone of Escondido Mountain (Table 2C) along the Mogollon-Datil fringe of the Chuska erg (Fig. 1) are volcaniclastic sandstones derived largely from Mogollon-Datil volcanic sources. Many of the quartz grains are limpid volcanic quartz of bipyramidal morphology with sharp extinction, and some of the K-feldspar grains are volcanic sanidine with low optic axial angle (2V). The variable quartz-feldspar contents of the Escondido Mountain samples may partly reflect mixing with arkosic sand of the type dominant in the central Chuska erg (Fig. 4). This postulate is supported by the occurrence of common plutonic quartz with undulatory extinction and of microcline in the more quartzo-feldspathic Escondido Mountain samples. Com-

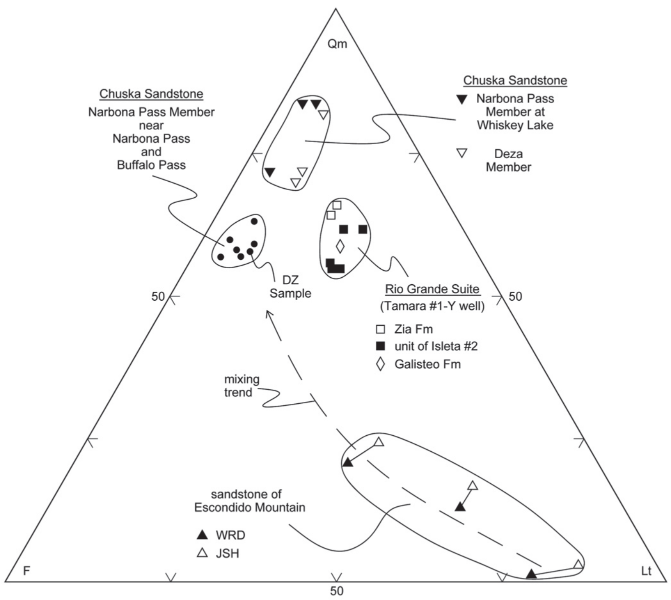

FIGURE 4. Petrofacies of the Chuska erg and associated strata (data from Table 2 except JSH data points from Chamberlin and Harris, 1994). See Table 1 for grain-type symbols (F=K+P; Lt=Qp+Lsm+Lvm).

TABLE 1. Detrital mode of detrital-zircon sandstone sample from Narbona Pass Member of Chuska Sandstone. See appendix for sample locality. Based on point count of 400 framework grains in thin section. Standard deviation (±) of counting error after Van der Plas and Tobi (1965).

Percentage	Symbol	Description
58 (± 2.5)	Qm	monocrystalline quartz: most with the equant shapes and undulatory extinction of common plutonic quartz; some with the even extinction and elongate habit of metamorphic quartz; none with the limpid quality, bipyramidal habit, or sharp extinction of volcanic quartz
23 (± 2.1)	K	monocrystalline K-feldspar: approximately half is microcline definitively indicative of plutonic derivation and the remainder is orthoclase of permissively plutonic derivation
11 (± 1.6)	P	monocrystalline plagioclase feldspar: much but not all is twinned but little if any is visibly zoned, implying derivation mainly from plutonic and metamorphic basement rocks
3 (± 0.9)	Qp	polycrystalline quartzose lithic fragments: dominantly microcrystalline chert or metachert but traces of foliated metaquartzite also present
3 (± 0.9)	Lsm	polycrystalline sedimentary-metasedimentary lithic fragments: microgranular clastic or metaclastic varieties dominant, but traces of foliated tectonite (slate or phyllite) and murky argillite also present; metasedimentary probably dominant over sedimentary sources
2 (± 0.7)	Lvm	polycrystalline volcanic-metavolcanic lithic fragments: microlitic and felsitic varieties subequal in abundance; derivation mainly from altered or metamorphosed source rocks implied by lack of pristine fabrics or original volcanic mineralogy

parisons of K-feldspar contents and P/F ratios (Table 2C) with the Chuska arkosic petrofacies (Table 2A) allows admixture of as much as 10%-25% arkosic sand into the more quartzo-feldspathic Escondido Mountain samples. The double points plotted on Figure 4 for sandstone of Escondido Mountain represent independent point counts of the same thin sections by WRD and J.S. Harris (JSH; Chamberlin and Harris, 1994), and provide a visual impression of the degree of uncertainty introduced into modal data by operator variance. Both sets of counts, however, reveal the Escondido Mountain samples to be lithic sands unlike other remnants of the Chuska erg.

Samples of the unit of Isleta #2 from the subsurface of the Rio Grande rift (Tamara #1-Y well) at the eastern edge of the Chuska erg plot within a discrete field in QmFLt space (Fig. 4) that includes subsurface samples from underlying (Galisteo) and overlying (Zia) formations (Table 2; Fig. 2). The Rio Grande suite of samples has a distinctly higher Lt/F ratio (Fig. 4) than the arkosic petrofacies of the central Chuska erg, and evidently derives from nearby sources that contributed to pre-erg and post-erg strata as well as to the fringe of the Chuska erg. Perhaps the arkosic sand blown into the central Chuska erg from the west (Fig. 1) never reached its eastern fringe near the Rio Grande rift. There is no hint from the modal data for admixture of arkosic sand from the central Chuska erg into the erg-fringe sands now structurally down-dropped within the Rio Grande rift.

CHUSKA ERG ANATOMY

The variability of sandstone petrofacies within the Chuska erg implies either variable pathways for eolian sand transport across and within the Chuska erg or segmentation of the Chuska erg, or both. The paleowind direction across the Chuska erg (Fig. 1) permits the arkosic petrofacies of the erg remnant forming the Narbona Pass Member of the Chuska Sandstone in the northern and central Chuska Mountains (Buffalo Pass and Narbona Pass) to reflect systematic deflation of piedmont alluvium derived from Precambrian basement of central Arizona, without the same sediment feed affecting eolian deposition along southern and eastern flanks of the erg where volcaniclastic and quartzolithic petrofacies are dominant, respectively (Table 2; Fig. 4). The presence of a more quartzose eolian petrofacies forming the Narbona Pass Member of the Chuska Sandstone in the southern Chuska Mountains (Whiskey Lake) is compatible with the postulate of multiple sand pathways across the erg (Table 2A), as there are no paleogeographic barriers separating our sample sites in the Chuska Mountains. The similarity of the quartzose eolian petrofacies at Whiskey Lake to the petrofacies of the underlying fluvial Deza Member of the Chuska Sandstone may indicate that fluvial deposits derived from Precambrian sources in central Arizona did not form the sole sedimented surface deflated to feed sand into the Chuska erg. Further sampling and analysis will be required to document the full petrofacies variability within the broad expanse of the erg as it existed before most of it was removed by erosion.

Our petrographic data suggest that the Chuska erg may have been subdivided into segments of different petrofacies by inselbergs that rose locally above its surface, at least during early phases of erg sedimentation. The base of the Chuska Sandstone in the Chuska Mountains lies at elevations of 2350-2415 m, and its top surface may not have exceeded ~3000 m (Fig. 5). Present elevations at the crests of the Carrizo Mountains to the north and the Zuni Mountains to the south reach ~2850 m, higher than the base of erg deposits in the intervening Chuska Mountains even without allowing for post-Oligocene erosion. Paleotopography along the base of the erg accumulation may have influenced sand transport across the erg surface during erg evolution. Peak elevations in the volcanic fields that surrounded the Chuska erg on three sides remain higher than remnants of the Chuska erg despite post-Oligocene erosion. The present highest elevations of Precambrian bedrock in central Arizona are as low, however, as the base of Chuska erg deposits. These low elevations of the inferred

TABLE 2. Modal compositions of Chuska eolianites and related strata. See Table 1 and Figure 4 for symbols of grain types (left column; Qt=Qm+Qp; F=P+K; L=Lsm+Lvm; Lt+L+Qp). Asterisk denotes detrital zircon sample (Table 1; Appendix).

A. Narbona Pass Member of Chuska Sandstone, Chuska Mountains

	Buffalo Pass			Narbona Pass				Whiskey Lake		
	BP-1	BP-2	BP-3	NARCHU*	TCCRY3	NAR1	NAR2	WL-1	WL-2	WL-3
Qm	63	60	57	58	59	58	57	84	72	84
Qp	3	1	2	3	3	2	3	1	3	3
(*Qt*)	*66*	*61*	*59*	*61*	*62*	*60*	*60*	*85*	*75*	*87*
K	24	28	28	23	25	26	27	11	19	8
P	7	8	11	11	8	10	9	2	5	2
(*F*)	*31*	*36*	*39*	*34*	*33*	*36*	*36*	*13*	*24*	*10*
Lsm	2	1	1	3	2	2	2	1	tr	1
Lvm	1	2	1	2	3	2	2	1	tr	1
(*L*)	*3*	*3*	*2*	*5*	*5*	*4*	*4*	*2*	*1*	*2*
(*Lt*)	*6*	*4*	*4*	*8*	*8*	*6*	*7*	*3*	*4*	*5*

	B. Deza Member (fluvial) of Chuska Sandstone			C. sandstone of Escondido Mountain (eolian)		
	basal	TDCRY1	transitional	KC2	#19	#20
Qm	82	70	69	21	10	1
Qp	2	2	3	4	1	0
(*Qt*)	*84*	*72*	*72*	*25*	*11*	*1*
K	8	16	14	6	3	0
P	3	5	5	32	17	20
(*F*)	*11*	*21*	*19*	*38*	*20*	*20*
Lsm	3	4	5	1	0	0
Lvm	2	3	4	36	69	79
(*L*)	*5*	*7*	*9*	*37*	*69*	*79*
(*Lt*)	*7*	*9*	*12*	*41*	*70*	*79*

D. Subsurface strata of Tamara #1-Y well, Rio Grande rift (figures are depth of cuttings in feet below well collar)

	Zia Formation		unit of Isleta #2 (Chuska erg)					Galisteo
	1390-1420	2620-50	3970-4000	4150-80	5020-50	5230-60	5290-5320	5410-40
Qm	64	66	62	62	55	56	55	59
Qp	3	5	5	2	7	3	5	6
(*Qt*)	*67*	*71*	*67*	*64*	*62*	*59*	*60*	*65*
K	16	14	10	13	16	16	13	15
P	3	3	5	5	7	7	9	5
(*F*)	*19*	*17*	*15*	*18*	*23*	*23*	*22*	*20*
Lsm	11	8	6	7	9	10	8	6
Lvm	3	4	12	11	6	8	10	9
(*L*)	*14*	*12*	*18*	*18*	*15*	*18*	*18*	*15*
(*Lt*)	*17*	*17*	*23*	*20*	*22*	*21*	*23*	*21*

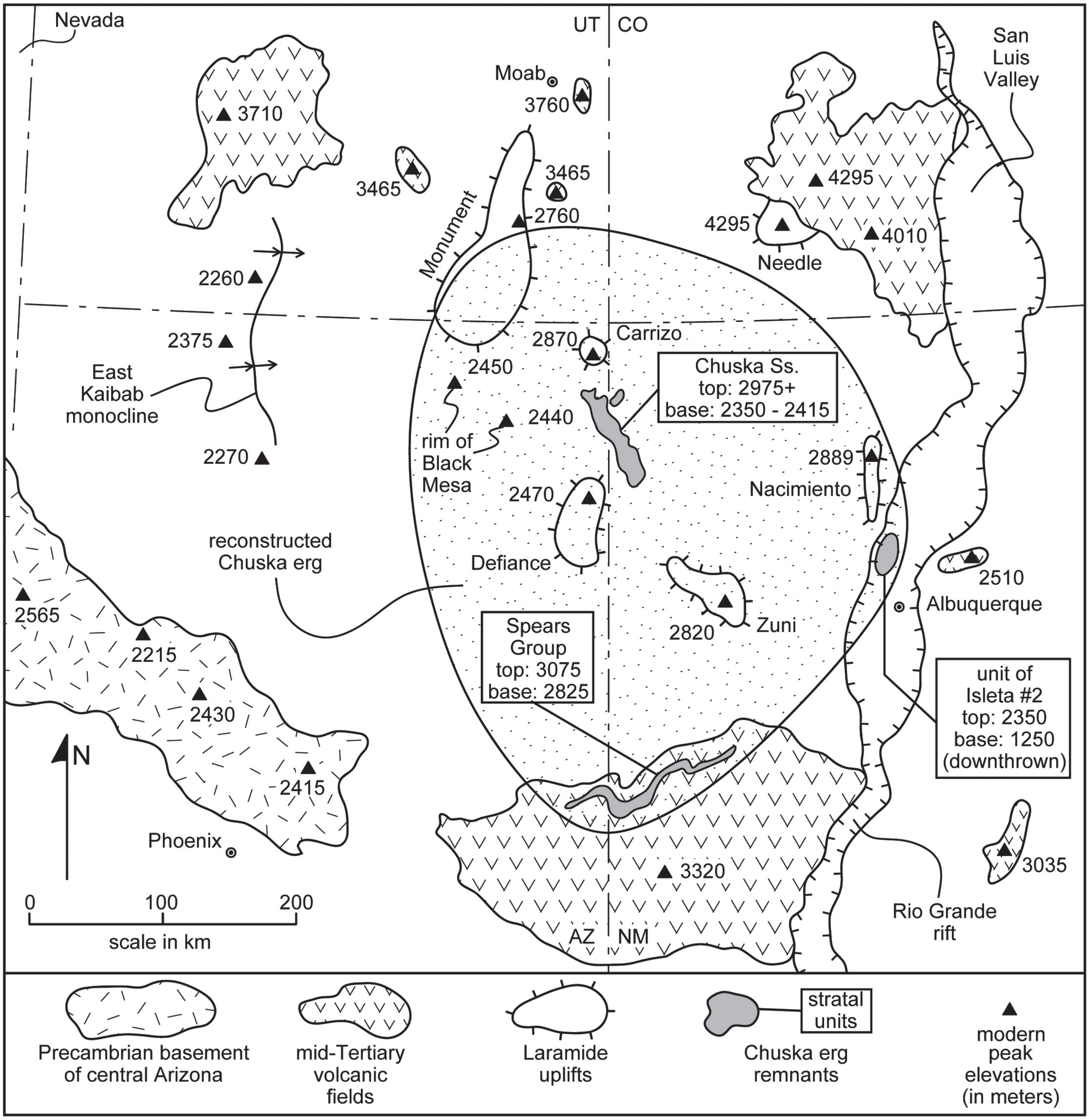

FIGURE 5. Present elevations in meters of the base and top of Chuska erg deposits and of salient peaks formed by pre-Chuska bedrock or Oligocene volcanic rocks.

provenance for the Chuska arkosic petrofacies suggest either that the piedmont fluvial deposits deflated to feed the Chuska erg stood at a lower elevation than the erg itself, or that significant post-Oligocene erosion or subsidence has lowered the ambient elevation of Precambrian outcrops in central Arizona. The current elevations of all topographic features both inside and outside the confines of the Chuska erg may have been affected by Neogene deformation that was not taken into account for preparation of Figure 5 (e.g., Moucha et al., 2008; Karlstrom et al., 2008).

The petrographic contrasts among the three eolian sandstone units treated here as remnants of the Chuska erg permit the alternate interpretation that each represents a separate dune field, but that conclusion would conflict with arguments, based on analogy with the morphology of modern ergs, that all are remnants of a single Chuska erg of regional extent (Cather et al., 2008).

CONCLUSIONS

Zircon U-Pb ages indicate that the overwhelming majority of detrital zircons in the arkosic petrofacies of the eolian Narbona Pass Member of the Chuska Sandstone near Narbona Pass in the Chuska Mountains were ultimately derived from Precambrian bedrock of central Arizona. The arkosic sand was presumably transported northward from the central Arizona provenance to form a piedmont ramp of fluvial deposits lying up-paleowind from the Chuska erg. Systematic deflation of the alluvium then fed arkosic sand into the Chuska erg. Petrographic study indicates, however, that other eolianite remnants of the Chuska erg in the southernmost Chuska Mountains, along the northern fringe of the Mogollon-Datil volcanic field, and in the subsurface of the Rio Grande rift contain quartzose, volcaniclastic, and quartzolithic sands, respectively, of different and mutually contrasting provenances for which the detrital zircons in the arkosic petrofacies provide no information.

ACKNOWLEDGMENTS

Permission to collect samples of the Chuska Sandstone was granted by the Navajo Nation, and U-Pb dating of detrital zircons at the Arizona LaserChron Center was supported by National Science Foundation Grants EAR-0341987 and EAR-0443387. We thank R.M. Chamberlin and S.D. Connell for the loan of thin sections from the sandstone of Escondido Mountain and the subsurface unit of Isleta #2, respectively. Figures were prepared by Jim Abbott of SciGraphics. Reviews by L.J. Crossey and S.G. Lucas improved the paper.

REFERENCES

Cather, S.M., Peters, L., Dunbar, N.W., and McIntosh, W.C., 2003, Genetic stratigraphy, provenance, and new age constraints for the Chuska Sandstone (Upper Eocene–Lower Oligocene), New Mexico–Arizona: N. M. Geological Society, 54th Field Conference Guidebook, p. 397-412.

Cather, S.M., Connell, S.D., Chamberlin, R.M., McIntosh, W.C., Jones, G.E., Potochnik,A.R., Lucas, S.G., and Johnson, P.S., 2008, The Chuska erg: Paleogeomorphic and paleoclimatic implications of an Oligocene sand sea on the Colorado Plateau: Geological Society of America Bulletin, v. 120, p. 13-33.

Chamberlin, R.M., and Harris, J.S., 1994, Upper Eocene and Oligocene volcaniclastic sedimentary stratigraphy of the Quemado-Escondido Mountain area, Catron County, New Mexico: N. M. Geological Society, 45th Field Conference Guidebook, p. 269-275.

Cumella, S.P., 1983, Relation of Upper Cretaceous regressive sandstone units of the San Juan basin to source area tectonics, in Reynolds, M.W., and Dolly, E.D., eds., Mesozoic paleogeography of the west-central United States: Denver, Society of Economic Paleontologists and Mineralogists Rocky Mountain Paleogeography Symposium 2, p. 189-199.

Dickinson, W.R., 1985, Interpreting provenance relations from detrital modes of sandstones, *in* Zuffa, G.G., ed., Provenance of arenites: Dordrecht, Reidel, p. 333-361.

Dickinson, W.R., and Gehrels, G.E., 2008a, U-Pb ages of detrital zircons in relation to paleogeography: Triassic paleodrainage networks and sediment dispersal across southwest Laurentia: Journal of Sedimentary Research, v. 78, p. 746-754.

Dickinson, W.R., and Gehrels, G.E., 2008b, Sediment delivery to the Cordilleran foreland basin: Insights from U-Pb ages of detrital zircons in Upper Jurassic and Cretaceous strata of the Colorado Plateau: American Journal of Science, v. 308, p. 1041-1082.

Dickinson, W.R., and Gehrels, G.E., 2009a, U-Pb ages of detrital zircons in Jurassic eolian and associated sandstones of the Colorado Plateau: Evidence for transcontinental dispersal and intraregional recycling of sediment: Geological Society of America Bulletin, v. 121, p. 408-433.

Dickinson, W.R., and Gehrels, G.E., 2009b, Provenance interpretations from U-Pb ages of detrital zircons (abs): New Mexico Geology, v. 31, p. 45-46.

Dickinson, W.R., Gehrels, G.E., and Cather, S.M., 2009a, U-Pb ages of detrital zircons from the Oligocene Chuska Sandstone (Arizona–New Mexico): Implications for sand provenance (abs): New Mexico Geology, v. 31, p. 46.

Dickinson, W.R., Lawton, T.F., and Gehrels, G.E., 2009b, Recycling detrital zircons: A case study from the Cretaceous Bisbee Group of southern Arizona: Geology, v. 37, p. 503-506.

Eichler, C.M., and McGraw, J.L., 2008, U-Pb ages of detrital zircons from sandstone of the Oligocene Chuska Formation, northwestern New Mexico (abs): Geological Society of America Abstracts With Programs, v. 40, no.1, p. 57.

Gehrels, G.E., Valencia, V.A., and Ruiz, J., 2008, Enhanced precision, accuracy, efficiency, and spatial resolution of U-Pb ages by laser ablation–multicollector–inductively coupled plasma–mass spectrometry. Geochemistry Geophysics Geosystems, v. 9, no. 3, Q03017, 13 p.

Karlstrom, K.E., Bowring, S.A., and Conway, C.M., 1987, Tectonic significance of an Early Proterozoic two-province boundary in central Arizona: Geological Society of America Bulletin, v. 99, p. 529-538.

Karlstrom, K.E., Crow, R., Crossey, L.J., Coblentz, D., and Van Wijk, J.W., 2008, Model for tectonically driven incision of the younger than 6 Ma Grand Canyon: Geology, v. 36, p. 835-838.

Lancaster, N., and Ollier, C.D., 1983, Sources of sand for the Namib sand sea: Zeitschrift für Geomorphologie, v. 45, p. 71-83.

Ludwig, K.R., 2003, Isoplot 3.00: Berkeley, California Geochronology Center Special Publication No. 4, 70 p.

Lucas, S.G., and Cather, S.M., 2003, Stratigraphy of the Chuska Sandstone, New Mexico–Arizona: N. M. Geological Society 54th Field Conference Guidebook, p. 389-395.

Madole, R.F., Romig, J.H., Aleinikoff, J.N., VanSistine, D.P., and Yacob, E.Y., 2007, On the origin and age of the Great Sand Dunes, Colorado: Geomorphology, v. 99, p. 99-119.

Moucha, R., Forte, A.M., Rowley, D.B., Mitrovica, J.X., Simmona, N.A., and Grand, S.P., 2008, Mantle convection and the recent evolution of the Colorado Plateau and the Rio Grande Rift valley: Geology, v. 36, p. 439-442.

Muhs, D.R., Reynolds, R.L., Been, J., and Skipp, G., 2003, Eolian sand transport pathways in the southwestern United States: Importance of the Colorado River and local sources: Quaternary International, v. 104, p. 3-18.

Pell, S.D., Williams, I.S., and Chivas, A.R., 1997, The use of protolith zircon-age fingerprints in determining the protosource areas for some Australian dune sands: Sedimentary Geology, v. 109, p. 233-260.

Press, W.H., Flannery, B.P., Tenkolsky, S.A., and Vetterling, W.T., 1986, Numerical recipes: Cambridge University Press, 818 p.

Shaw, C.A., and Karlstrom, K.E., 1999, The Yavapai–Mazatzal crustal boundary in the southern Rocky Mountains: Rocky Mountain Geology, v. 34, p. 37-52.

Van der Plas, L., and Tobi, A.C., 1965, A chart for determining the reliability of point counting results: American Journal of Science, v. 263, p. 87-90.

Wasson, R.J., Rajaguru, S.N., Misra, V.N., Agrawal, D.P., Dhir, R.P., Sengjivi, A.K., and Kameswara, K., 1983, Geomorphology, late Quaternary stratigraphy and paleoclimatology of the Thar dunefield: Zeitschift für Geomorphologie, v. 45, p. 117-151.

Whitmeyer, S.J., and Karlstrom, K.E., 2007, Tectonic model for the Proterozoic growth of North America: Geosphere, v. 3, p. 220-259.

Wiegand, J.P., 1977, Dune morphology and sedimentology at Great Sand Dunes National Monument [M.S. Thesis]: Fort Collins, Colorado State University, 165 p.

APPENDIX: U-Pb geochronological analyses for individual detrital zircon grains in Narbona Pass Member of Chuska Sandstone at high roadcut 0.9 miles west of crest of Narbona Pass on north side of New Mexico Highway 134 (GPS: 36°05.234' N, 108°108.594' W); 206Pb/204Pb (not listed) used for common-lead correction to obtain isotopic ratios involving 206Pb* and 207Pb* (radiogenic lead).

Isotope Ratios						Apparent Ages (Ma)						Best Ages (Ma)	
206Pb* 207Pb*	± (%)	207Pb* 235U	± (%)	206Pb* 238U	± (%)	206Pb* 238U*	± (Ma)	207Pb* 235U	± (Ma)	206Pb* 207Pb*	± (Ma)	Best age (Ma)	± (Ma)
20.3271	15.8	0.1711	15.9	0.0252	1.0	160.6	1.6	160.4	23.6	157.1	372.9	160.6	1.6
20.8381	7.2	0.1811	7.2	0.0274	1.0	174.0	1.7	169.0	11.3	98.7	169.5	174.0	1.7
19.7517	1.9	0.2485	2.2	0.0356	1.0	225.5	2.2	225.4	4.4	223.9	44.5	225.5	2.2
18.8916	3.5	0.4286	3.6	0.0587	1.0	367.9	3.6	362.2	11.1	325.9	79.3	367.9	3.6
16.7762	3.0	0.8022	3.3	0.0976	1.5	600.4	8.6	598.1	15.1	589.4	64.7	600.4	8.6
13.5723	1.7	1.7031	2.5	0.1676	1.9	999.1	17.2	1009.7	16.1	1032.7	34.4	1032.7	34.4
13.0187	1.0	2.0048	1.9	0.1893	1.6	1117.6	16.2	1117.1	12.7	1116.3	20.0	1116.3	20.0
12.9338	2.1	1.7752	2.8	0.1665	1.9	992.9	17.5	1036.4	18.3	1129.3	41.2	1129.3	41.2
11.6008	1.0	2.5735	1.4	0.2165	1.0	1263.5	11.5	1293.1	10.3	1342.7	19.3	1342.7	19.3
11.3078	1.8	2.9277	2.1	0.2401	1.2	1387.2	15.1	1389.1	16.2	1391.9	33.8	1391.9	33.8
11.2557	1.3	2.9389	1.8	0.2399	1.3	1386.2	16.2	1392.0	13.7	1400.8	24.2	1400.8	24.2
11.2365	2.0	3.0356	2.3	0.2474	1.0	1425.0	12.8	1416.6	17.4	1404.1	39.1	1404.1	39.1
11.2290	1.0	2.9867	1.6	0.2432	1.3	1403.5	15.9	1404.2	12.2	1405.3	19.2	1405.3	19.2
11.2223	2.9	2.9474	3.4	0.2399	1.9	1386.1	23.1	1394.2	25.9	1406.5	55.0	1406.5	55.0
11.2085	1.1	2.8966	1.9	0.2355	1.5	1363.1	18.4	1381.0	14.1	1408.8	21.3	1408.8	21.3
11.1954	1.5	3.0677	1.8	0.2491	1.0	1433.8	12.9	1424.7	13.7	1411.1	28.3	1411.1	28.3
11.1922	1.0	2.9258	1.4	0.2375	1.0	1373.7	12.6	1388.6	10.8	1411.6	19.1	1411.6	19.1
11.1269	1.2	2.9382	1.6	0.2371	1.1	1371.7	13.6	1391.8	12.1	1422.8	22.2	1422.8	22.2
11.0855	1.2	2.6524	1.7	0.2133	1.3	1246.1	14.7	1315.3	12.8	1429.9	22.1	1429.9	22.1
11.0792	1.2	3.0348	2.2	0.2439	1.8	1406.7	23.1	1416.4	16.8	1431.0	23.3	1431.0	23.3
11.0407	1.3	3.0390	2.9	0.2434	2.7	1404.1	33.4	1417.5	22.5	1437.6	24.2	1437.6	24.2
10.9525	1.3	3.1842	1.7	0.2529	1.1	1453.6	14.7	1453.3	13.5	1452.9	25.3	1452.9	25.3
10.9275	1.5	3.0643	2.9	0.2429	2.5	1401.6	31.4	1423.8	22.3	1457.3	28.5	1457.3	28.5
10.6391	1.3	3.2316	2.4	0.2494	2.0	1435.2	26.0	1464.8	18.7	1507.9	24.7	1507.9	24.7
10.3189	1.3	3.5789	2.0	0.2678	1.5	1529.8	20.6	1544.9	15.6	1565.4	23.6	1565.4	23.6
9.9158	1.0	3.9665	1.5	0.2853	1.1	1617.8	15.9	1627.4	12.1	1639.8	18.6	1639.8	18.6
9.8672	2.2	3.9494	2.4	0.2826	1.0	1604.6	14.2	1623.9	19.4	1648.9	40.2	1648.9	40.2
9.8410	1.9	3.9426	2.5	0.2814	1.7	1598.4	23.4	1622.5	20.5	1653.8	35.7	1653.8	35.7
9.8094	1.7	4.0998	2.0	0.2917	1.1	1649.9	15.7	1654.3	16.3	1659.8	31.1	1659.8	31.1
9.8060	2.0	3.9355	2.3	0.2799	1.0	1590.8	14.1	1621.0	18.3	1660.4	37.4	1660.4	37.4
9.7749	1.0	4.0893	1.5	0.2899	1.1	1641.1	15.6	1652.2	12.0	1666.3	18.6	1666.3	18.6
9.7727	1.3	4.0372	2.0	0.2861	1.5	1622.2	21.8	1641.7	16.3	1666.7	24.2	1666.7	24.2
9.7649	1.0	4.1182	1.4	0.2917	1.0	1649.8	14.6	1657.9	11.6	1668.2	18.5	1668.2	18.5
9.7597	1.1	3.9400	4.0	0.2789	3.9	1585.8	54.4	1621.9	32.5	1669.2	19.6	1669.2	19.6
9.7506	1.8	4.2520	2.6	0.3007	1.9	1694.7	28.2	1684.1	21.4	1670.9	33.1	1670.9	33.1
9.7371	1.6	4.0760	1.9	0.2879	1.0	1630.8	14.4	1649.5	15.4	1673.5	29.6	1673.5	29.6
9.7289	1.0	3.9992	1.4	0.2822	1.0	1602.4	14.2	1634.0	11.5	1675.0	18.5	1675.0	18.5
9.7185	1.0	4.0894	1.5	0.2882	1.1	1632.8	16.2	1652.2	12.3	1677.0	18.5	1677.0	18.5
9.7117	1.7	4.0842	2.0	0.2877	1.1	1629.9	15.4	1651.2	16.7	1678.3	32.1	1678.3	32.1
9.7111	1.4	4.2913	1.9	0.3022	1.3	1702.4	18.7	1691.7	15.3	1678.4	25.3	1678.4	25.3
9.6889	1.0	4.0493	2.0	0.2845	1.7	1614.2	24.0	1644.2	15.9	1682.6	18.5	1682.6	18.5
9.6883	1.9	4.2008	2.7	0.2952	1.8	1667.3	26.7	1674.2	21.8	1682.7	35.8	1682.7	35.8
9.6790	1.8	4.1479	2.7	0.2912	1.9	1647.4	28.1	1663.8	21.7	1684.5	33.6	1684.5	33.6
9.6723	1.3	3.9488	1.6	0.2770	1.0	1576.3	14.0	1623.7	13.0	1685.8	23.1	1685.8	23.1
9.6722	1.5	3.9860	2.1	0.2796	1.5	1589.4	20.4	1631.3	17.1	1685.8	28.2	1685.8	28.2
9.6687	1.2	4.3089	1.6	0.3022	1.0	1702.0	15.0	1695.1	12.9	1686.5	22.1	1686.5	22.1
9.6571	1.0	4.2496	1.4	0.2976	1.0	1679.6	14.8	1683.7	11.6	1688.7	18.5	1688.7	18.5

9.6538	1.5	4.1230	2.1	0.2887	1.4	1634.9	20.8	1658.9	17.1	1689.3	28.0	1689.3	28.0
9.6535	1.0	4.0581	1.4	0.2841	1.0	1612.1	14.3	1645.9	11.5	1689.4	18.4	1689.4	18.4
9.6535	2.4	4.3154	2.8	0.3021	1.4	1701.9	21.4	1696.3	22.7	1689.4	43.4	1689.4	43.4
9.6517	1.5	4.2050	2.0	0.2944	1.4	1663.2	20.2	1675.0	16.7	1689.7	27.7	1689.7	27.7
9.6416	1.2	4.0596	1.6	0.2839	1.0	1610.9	14.3	1646.2	12.9	1691.7	22.5	1691.7	22.5
9.6287	1.6	4.3500	1.9	0.3038	1.0	1710.0	15.0	1702.9	15.6	1694.1	29.7	1694.1	29.7
9.6260	1.1	4.2609	1.8	0.2975	1.5	1678.8	22.0	1685.8	15.0	1694.7	19.5	1694.7	19.5
9.6113	1.4	4.1504	1.8	0.2893	1.1	1638.1	15.9	1664.3	14.6	1697.5	26.0	1697.5	26.0
9.6110	1.1	4.1445	1.7	0.2889	1.3	1636.0	18.2	1663.1	13.6	1697.5	19.9	1697.5	19.9
9.6087	1.0	4.2951	2.2	0.2993	1.9	1688.0	28.8	1692.4	18.1	1698.0	19.2	1698.0	19.2
9.6013	2.1	3.6546	6.0	0.2545	5.6	1461.6	73.6	1561.5	47.9	1699.4	38.7	1699.4	38.7
9.5842	1.5	4.1376	1.8	0.2876	1.1	1629.6	15.7	1661.8	15.0	1702.7	27.3	1702.7	27.3
9.5777	1.4	4.3098	2.1	0.2994	1.6	1688.2	23.0	1695.2	17.1	1703.9	25.4	1703.9	25.4
9.5255	1.0	4.3044	1.6	0.2974	1.2	1678.3	17.7	1694.2	13.1	1714.0	19.1	1714.0	19.1
9.5203	1.7	4.2772	2.3	0.2953	1.5	1668.1	22.0	1689.0	18.8	1715.0	31.8	1715.0	31.8
9.5015	1.7	4.3590	2.2	0.3004	1.4	1693.2	20.5	1704.6	17.9	1718.6	30.7	1718.6	30.7
9.4903	1.1	4.3056	1.6	0.2964	1.3	1673.2	18.6	1694.4	13.5	1720.8	19.3	1720.8	19.3
9.4893	1.0	4.2300	1.4	0.2911	1.0	1647.1	14.5	1679.9	11.6	1721.0	18.4	1721.0	18.4
9.4820	1.0	4.3180	1.5	0.2969	1.1	1676.1	15.5	1696.8	12.0	1722.4	18.4	1722.4	18.4
9.4776	1.3	4.2500	2.4	0.2921	2.1	1652.2	30.0	1683.7	20.1	1723.2	24.2	1723.2	24.2
9.4727	1.5	4.3981	1.8	0.3022	1.0	1702.0	15.0	1712.0	14.8	1724.2	27.2	1724.2	27.2
9.4578	1.3	4.2419	1.8	0.2910	1.3	1646.4	18.3	1682.2	14.7	1727.1	23.3	1727.1	23.3
9.4396	1.1	4.4800	1.8	0.3067	1.3	1724.5	20.3	1727.3	14.6	1730.6	20.9	1730.6	20.9
9.4333	2.5	4.5501	2.7	0.3113	1.0	1747.1	15.3	1740.2	22.3	1731.8	45.5	1731.8	45.5
9.4050	1.4	4.3904	2.0	0.2995	1.3	1688.7	19.8	1710.5	16.2	1737.3	26.4	1737.3	26.4
9.4003	1.0	4.2620	1.5	0.2906	1.1	1644.4	15.5	1686.1	12.0	1738.3	18.3	1738.3	18.3
9.3898	1.8	4.4075	2.7	0.3002	2.0	1692.1	30.1	1713.8	22.6	1740.3	33.5	1740.3	33.5
9.3869	1.8	3.6140	3.8	0.2460	3.4	1418.0	43.5	1552.6	30.6	1740.9	32.3	1740.9	32.3
9.3855	2.6	4.3390	3.5	0.2954	2.4	1668.2	35.3	1700.8	29.0	1741.2	47.1	1741.2	47.1
9.3806	2.3	4.2560	3.0	0.2896	1.9	1639.3	27.1	1684.9	24.6	1742.1	42.9	1742.1	42.9
9.3779	1.0	4.2821	1.4	0.2913	1.0	1647.8	15.0	1689.9	11.8	1742.6	18.3	1742.6	18.3
9.3695	1.4	4.4186	2.3	0.3003	1.9	1692.6	28.0	1715.8	19.3	1744.3	25.1	1744.3	25.1
9.3679	1.5	4.3901	1.8	0.2983	1.0	1682.7	14.8	1710.5	15.1	1744.6	28.0	1744.6	28.0
9.3541	1.8	4.3382	2.5	0.2943	1.7	1663.0	25.4	1700.6	20.4	1747.3	32.2	1747.3	32.2
9.3407	1.4	4.5599	2.2	0.3089	1.7	1735.3	25.1	1742.0	18.0	1749.9	25.4	1749.9	25.4
9.3387	1.5	4.1279	3.0	0.2796	2.6	1589.3	36.5	1659.8	24.3	1750.3	26.7	1750.3	26.7
9.3197	1.0	4.4411	1.4	0.3002	1.0	1692.3	14.9	1720.0	11.7	1754.0	18.3	1754.0	18.3
9.3157	2.1	4.3203	2.4	0.2919	1.2	1651.0	17.9	1697.2	19.7	1754.8	37.5	1754.8	37.5
9.3129	2.9	4.4869	3.1	0.3031	1.0	1706.5	15.0	1728.5	25.5	1755.4	53.1	1755.4	53.1
9.2975	1.7	4.3745	3.0	0.2950	2.4	1666.4	35.7	1707.5	24.7	1758.4	31.6	1758.4	31.6
9.2974	1.4	4.4929	2.2	0.3030	1.8	1706.0	26.4	1729.7	18.7	1758.4	25.6	1758.4	25.6
9.2699	1.8	4.7365	2.8	0.3184	2.1	1782.1	32.2	1773.7	23.2	1763.8	33.6	1763.8	33.6
9.2617	1.5	4.5050	2.3	0.3026	1.7	1704.2	25.8	1731.9	19.1	1765.5	28.0	1765.5	28.0
9.2590	1.4	4.5947	1.7	0.3085	1.0	1733.5	15.2	1748.3	14.4	1766.0	25.6	1766.0	25.6
9.2548	1.5	4.4563	1.9	0.2991	1.2	1686.9	17.1	1722.9	15.7	1766.8	27.6	1766.8	27.6
9.2473	2.6	4.1849	3.9	0.2807	3.0	1594.8	41.7	1671.1	32.1	1768.3	47.2	1768.3	47.2
9.2255	1.9	4.1220	2.3	0.2758	1.4	1570.2	18.8	1658.7	19.1	1772.6	34.7	1772.6	34.7
9.0021	1.6	4.9763	1.9	0.3249	1.0	1813.6	15.8	1815.3	16.1	1817.2	29.4	1817.2	29.4
8.9381	2.3	4.6516	2.9	0.3015	1.8	1698.9	26.3	1758.6	24.1	1830.2	41.3	1830.2	41.3
8.8756	1.3	5.2023	2.1	0.3349	1.7	1862.0	27.5	1853.0	18.2	1842.9	23.3	1842.9	23.3
8.2790	1.0	5.6700	1.6	0.3405	1.3	1888.8	21.1	1926.8	14.1	1967.9	17.8	1967.9	17.8
5.1165	1.7	14.5766	2.5	0.5409	1.9	2787.3	42.8	2788.0	23.9	2788.5	27.2	2788.5	27.2
5.0687	1.0	14.3123	1.4	0.5261	1.0	2725.2	22.2	2770.6	13.4	2803.9	16.4	2803.9	16.4